Time-lapse VSP reservoir monitoring

JOHN O'BRIEN, FIONA KILBRIDE, and FRANK LIM, Anadarko Petroleum, Houston, Texas, U.S.

Although 3D seismic imaging, based on surface sources and receivers, has been the primary tool used for geophysical reservoir monitoring to date, vertical seismic profiling (VSP) has characteristics that make this technique particularly suitable for time-lapse surveying. In particular, the use of downhole receivers provides some advantages:

- Increased frequency content improves vertical and lateral resolution, allowing us to examine the reservoir in greater detail, both statically and dynamically.
- Improved signal/noise ratio permits us to measure and quantify time-lapse changes in the reservoir with a high degree of confidence.

With the recent development of multilevel downhole arrays having 50 or more three-component geophones, we now have the capability of recording large 3D VSP surveys in a time-efficient manner. Such surveys generate high-quality and high-fidelity 3D images of the subsurface in the vicinity of the wellbore and provide a powerful tool for time-lapse imaging.

In this paper we present the results of a 3D VSP time-lapse imaging project in the Monell Unit of Patrick Draw Field, Wyoming, U.S. In 2001 Anadarko Petroleum initiated a miscible CO_2-enhanced oil recovery (EOR) pilot project in the Monell Unit. The objectives were to test the injection process and the response of the reservoir to CO_2 injection prior to start-up of a full-field CO_2 flood. As part of that project, movement of the CO_2 front in the reservoir was monitored by time-lapse 3D VSP; these results are presented in this paper. To the best of our knowledge, this is the first such 3D VSP reservoir monitoring application reported in the literature.

Monell Unit. The Monell Unit constitutes the southern portion of the Patrick Draw Field in south-central Wyoming (Figure 1). The reservoir interval is the Upper Almond UA-5 sandstone, the youngest sandstone member of the Upper Cretaceous Mesaverde group. The Upper Almond was deposited in a barrier island/tidal inlet channel setting, with predominantly north-south trending elongate barrier bars. The field is a stratigraphic trap; the reservoir pinches out updip into swamp and lagoonal shales and is overlain by the Lewis Shale.

The general dip of the reservoir is to the southeast at 4-5°. Due to the depositional environment, the reservoir is quite homogeneous, with little variation in thickness, porosity, or permeability. Little significant faulting has been identified from 3D seismic or from borehole correlations. Reservoir characteristics are summarized in Table 1.

The Monell Unit, which had an original-oil-in-place of 110 million bls, was initially produced under solution gas drive that yielded 24 million bls. The field was subsequently waterflooded and yielded an additional 16 million bls, leaving 70 million bls as a remaining target for enhanced oil recovery. Given the remaining oil-in-place, the homogeneous nature of the reservoir and its shallow depth, this field was identified as a strong candidate for EOR.

CO_2 pilot project. The Monell EOR program was initiated with a pilot project that consisted of a single five-spot pattern with a CO_2 injector at the center, two producing wells a quarter of a mile north and south of the injection well, and two water injectors a quarter of a mile to the east and west (Figure 2).

Figure 1. *Map showing the location of the pilot project.*

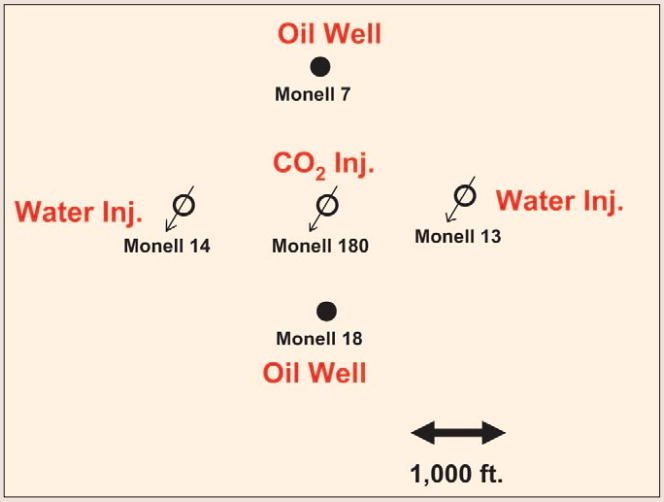

Figure 2. *Monell CO_2 EOR pilot project.*

Table 1. *Reservoir characteristics of Monell Unit, Patrick Draw Field, Wyoming, U.S.*

Average net thickness	25 ft
Porosity	20%
Permeability	30 mD
Depth	4800 ft
Oil gravity	43° API
Gas/oil ratio	500 scf/b
Original sw	46%
Present sw (before CO_2 flood)	67%
Reservoir pressure	2000 psi
Reservoir temperature	120° F

The water injectors were utilized to maintain reservoir pressure and to confine the CO_2 flood.

The CO_2 injector well, Monell 180 ST 1, is a nominally vertical well drilled specifically for the pilot project. A full suite of wireline logs was recorded in this well, including dipole sonic and density logs for geophysical analysis. This is the well

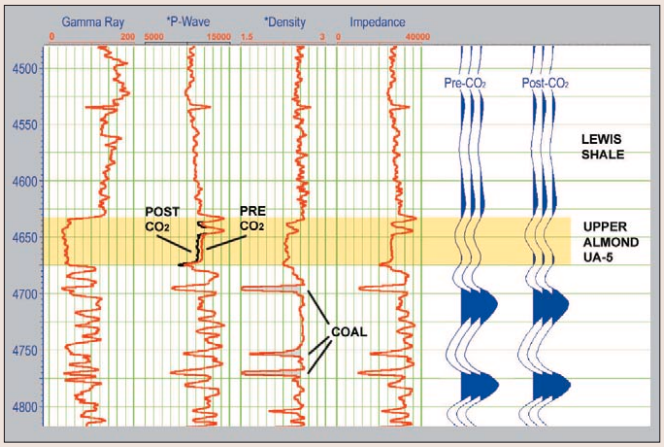

Figure 3. *Monell 180 ST 1 wireline log data. The Upper Almond UA-5 interval is the reservoir. The red curve on the P-velocity track shows the velocity before CO_2 injection and the black curve shows the computed velocity after injection, a difference of 700 ft/s. The seismic traces show 1D synthetic seismograms for both the preinjection and postinjection cases.*

Table 2. *Pore fluid saturation and average rock properties*

Pore fluid saturation			
	Brine	Oil	CO_2
Before CO_2 flood	67%	33%	—
After CO_2 flood	67%	16.5%	16.5%
Formation rock properties			
	P velocity (ft/s)	Density (gm/cc)	Acoustic impedance
Lewis Shale	11 000	2.55	28 000
UA-5 preflood	11 700	2.30	26 900
UA-5 postflood	11 000	2.30	25 300

**(Top) Pore fluid saturation for Upper Almond UA-5 sand before CO_2 flood as well as predicted saturations after flooding. (Bottom) Average rock properties for Lewis Shale and Upper Almond UA-5 sand. Rock properties for interval underlying the UA-5 reservoir are more complex, as discussed in the text.*

Table 3. *Acquisition parameters for the Monell baseline and monitor 3D VSP surveys*

Source locations	
Source line interval	500 ft
Source point interval	200 ft
Maximum offset (inline/Xline)	5000 ft
Number of VPs	1007
Seismic source	
Source type	Vibroseis
Sweep	8-180 Hz, linear sweep
Sweeps/VP	4
Sweep length	12 s
Receiver well	
Reservoir depth	4680 ft (MD)
Receiver array	
Number of levels	80
Geophone depths	405 - 4355 ft
Level spacing	50 ft
Geophones	15-Hz SM45, 3C pods

in which the VSP data were recorded.

The pilot project was launched in July 2001 with installation and testing of the oilfield equipment and of the injection processes. Continuous CO_2 injection commenced in January 2002, at which time the baseline 3D VSP survey was recorded. This provided a high-quality baseline image of the reservoir. Only minor amounts of CO_2, insufficient to affect the seismic response, had been injected prior to the baseline survey.

The pilot project continued in operation for an additional 18 months during which time a total of 430 million ft^3 of gas was injected at an average rate of 0.8 million ft^3/day. The pilot project was completed in June 2003 and the time-lapse monitor 3D VSP was then recorded.

Rock properties and seismic response. Prior to start-up of the pilot project, a study of the rock and fluid properties was performed to determine the time-lapse seismic response of the reservoir and to assess the feasibility of geophysical monitoring. Figure 3 shows the wireline log data for well Monell 180 ST 1, including the gamma ray, P-wave sonic and density logs, and the computed acoustic impedance. The reservoir interval occurs at a depth of 4633 ft in the well and is 42 ft thick, which is thicker than the field average of 25 ft and includes a thin (5 ft) tight streak.

The Upper Almond UA-5 is overlain by the relatively homogenous Lewis Shale. Log data recorded before CO_2 flooding show that the Upper Almond UA-5 sand has a higher velocity than the Lewis Shale but a lower density. The density contrast is greater than the velocity contrast and so the reservoir has lower acoustic impedance than the overlying shale. This interface is predicted to generate a trough on the seismic section according to the sign convention used throughout this paper, which is the reverse of the SEG polarity convention.

The Upper Almond UA-5 reservoir overlies a complex of sands, shales, and coals. The coals, although quite thin, have anomalously low acoustic impedance and so produce a strong seismic response. This is accentuated by the influence of the sands within this complex which are cemented and have relatively high acoustic impedance. The resulting effect is a significant degree of interference whereby the peak event corresponding to the base of the Upper Almond UA-5 is superimposed on the leading energy of the underlying reflections, thus masking the base of the reservoir.

The effect of CO_2 flooding on the rock properties has been estimated by application of the Biot-Gassmann equations for pore fluid substitution in the Upper Almond UA-5 (Table 2). These computations are based on an oil saturation of 33% before CO_2 flood and an estimated CO_2 sweep efficiency of 50%. Under these conditions we predict a decrease in P-wave velocity of 700 ft/s. (6%) in the sandstone due to CO_2 flooding and a negligible change in density.

Figure 3 includes 1D synthetic seismograms for both cases, before and after CO_2 flooding:

- Before CO_2 flooding, the reservoir seismic response consists of a trough doublet which overlies a strong peak; the upper trough corresponds to the top of the reservoir (Top UA-5) while the lower trough results from superposition of the base-of-reservoir (Base UA-5) and leading energy from the underlying reflections.
- After CO_2 flooding, the upper trough increases in amplitude by 30%. The interference pattern underlying this is

modified due to the increase in amplitude of the reflection from the base of the UA-5 sand.

These differences should be detectable using time-lapse 3D VSP acquired and processed properly, particularly the brightening of the trough event at the top of the reservoir. With this encouragement, a time-lapse 3D VSP program was designed and executed to monitor CO_2 movement in the reservoir during the pilot project.

3D VSP acquisition. For VSP data acquisition, the reservoir interval in Monell 180 ST 1 was isolated using a bridge plug. The borehole overlying the plug was then instrumented with an array of 80 3C geophones deployed over a depth of 4000 ft up to the near surface. Geophones were deployed on production tubing, within casing. The acquisition parameters are summarized in Table 3.

The survey was shot with a vibroseis source with a peak force of 62 000 lbs. Two vibroseis units were employed, shooting in ping-pong fashion. Based on in-field testing, a sweep frequency of 8-180 Hz was used for VSP acquisition.

Sources were on a rectangular grid with 500-ft spacing between shot lines and 200-ft spacing between shots along each line. Source locations extended 5000 ft from the geophone array in both inline and crossline directions, yielding a survey with full azimuthal coverage and with full offset coverage out to offsets equivalent to the depth of the target. A total of 1007 shots were recorded yielding a dataset in excess of 240 000 traces. Total recording time was less than 30 hours per survey. This provided a comprehensive measurement of the seismic wavefield, recorded efficiently in an operationally attractive short time.

As the goal of the project was to monitor changes in the reservoir, the baseline and monitor surveys were designed, acquired, and processed as consistently as feasible:

- Source points were reoccupied with an accuracy of ± 2 ft for 1000 of the 1007 shots.
- Receiver locations were reoccupied with an accuracy of ± 1/4 ft.
- Vibrator sweep parameters were repeated.
- Similar vibrator units were employed.
- An 80-level 3C geophone array was used for both surveys.

Both surveys used geophones of the same design and specifications; however, the baseline survey used a first-generation geophone array while the monitor survey used a re-engineered second-generation array which had better signal/noise characteristics. This was the largest difference in field acquisition between the two surveys.

3D VSP processing. To maintain consistency between the baseline and monitor surveys, the two were coprocessed through a common sequence with the same parameters, as summarized as follows:

1) Edit shots and assign geometry.
2) Hodogram analysis.
3) Determine geophone orientations.
4) Rotate data into uniform coordinate system.
5) Pick first breaks.
6) Compute shot statics separately for each survey (statics solutions for the two surveys agree within ± 1 ms).
7) Determine x,y locations of receivers based on first break traveltimes from a ring of shots around the well. (This shows a maximum difference of 42 ft relative to the conventional well deviation survey. The VSP-derived x,y locations were used in VSP processing)
8) Shot ensemble deterministic source signature-deconvolution.
9) Separate upgoing P-wavefield.
10) Radon filter to suppress downgoing shear-wave energy
11) Trace amplitude balance based on the amplitude of the P-wave direct arrival, followed by time-variant gain.
12) Test AGC to improve signal/noise ratio. (Baseline and monitor surveys were processed from this point forward both with and without AGC. Time-lapse differences were judged to be equivalent in both processing flows. As application of AGC results in a higher quality migrated image, the VSP sections shown in this paper include this AGC step in the processing flow.)
13) Generate a 1D velocity model by inverting first break times from near-offset shot records (The 1D profile was extended below the well using a constant velocity gradient.)
14) Extend the velocity model to 3D using the structural interpretation derived from well formation tops.
15) P-wave Kirchhoff prestack depth migration using source offsets of 0-5000 ft and dip aperture of 0-6° (This was deemed appropriate as structural dips in the image area are 4-5° with no significant faulting in the VSP image zone. The incidence angle aperture was limited to 0-25° to minimize anisotropy effects. The 3D VSP provides a high quality image of radius 1500 ft around the borehole at the Upper Almond level.)
16) Cross-equalization analysis. (The baseline and monitor migration volumes were analyzed for systematic differences in depth, phase, and amplitude gain. Only minor differences in depth and phase were observed. To compensate for these, a bulk static shift of 3 ft and a small spatially varying residual static and phase shift were applied. No gain adjustment was required.)
17) Spectral balance and amplitude envelope balance.
18) Generate time-lapse difference volumes.

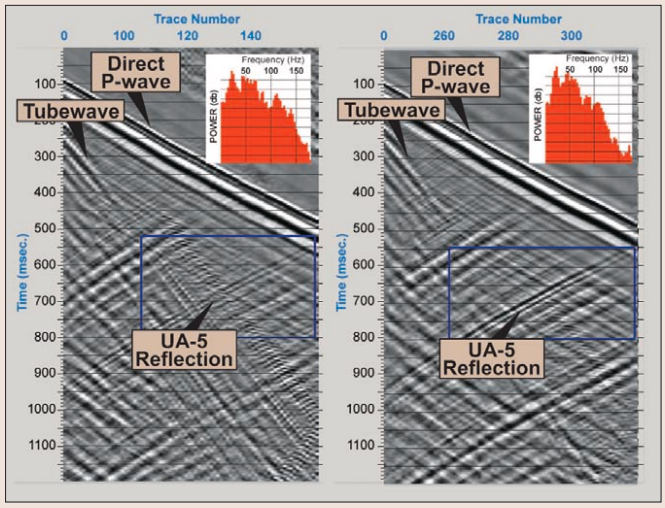

Figure 4. Comparison of collocated shots from the baseline survey (left) and monitor survey (right). Source offset = 406 ft. Figure shows vertical component data with AGC applied for display purposes. Inserts show the amplitude spectra of a data window including the Upper Almond UA-5 reflection. At near offsets the tube wave is stronger on the baseline survey than on the monitor but diminishes on both at larger source offsets.

The excellent match achieved between the baseline and monitor surveys, as indicated by the cross-equalization analysis, is attributed to the consistency in field acquisition and data processing.

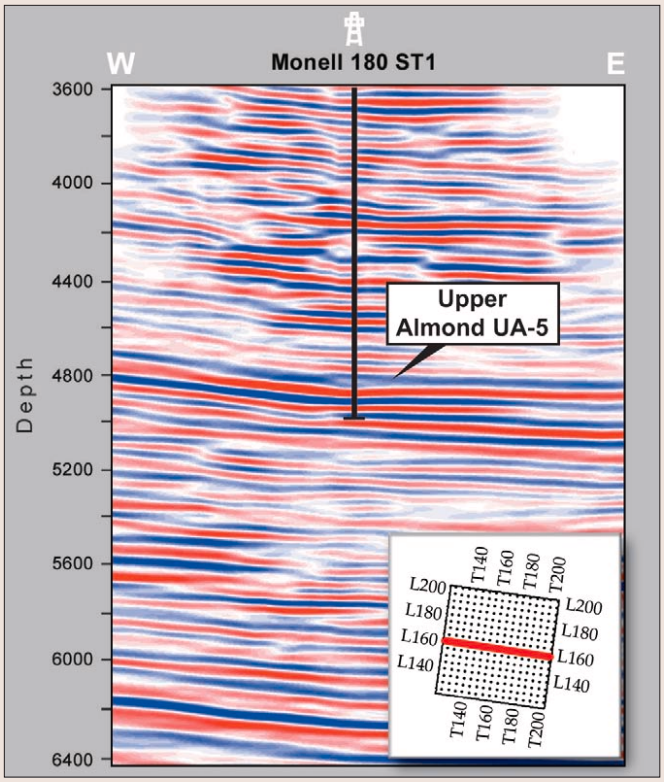

Figure 5. *East-west line from prestack depth-migrated baseline 3D VSP survey tying Monell 180 ST 1. The Upper Almond UA-5 is the blue trough doublet above the 4800-ft marker at the well.*

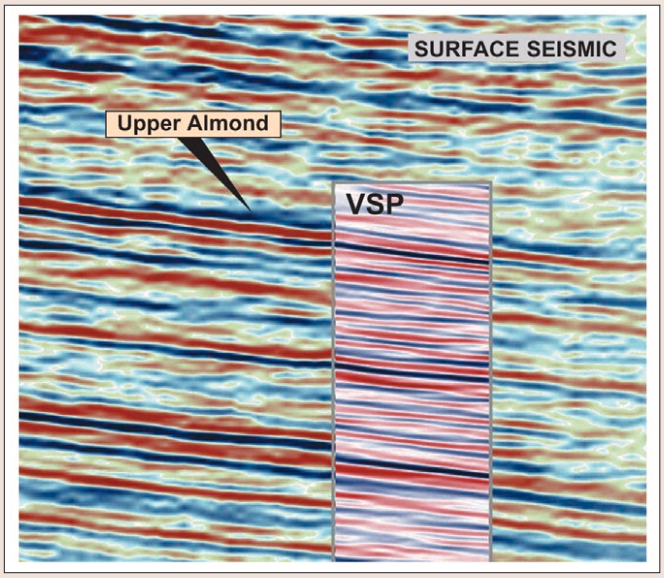

Figure 6. *Comparison of segment of Monell 3D VSP baseline survey (insert) and 3D surface seismic.*

VSP results. Figure 4 compares a set of collocated shots from the baseline and monitor surveys. The Upper Almond UA-5 reflection is clearly seen over the full geophone array. This comparison demonstrates the high quality and reproducibility of the survey. Figure 4 also shows amplitude spectra for a data window that includes the Upper Almond reflection, showing that the reflection data includes frequencies exceeding 130 Hz.

Figure 5 shows an east-west line from the fully processed baseline VSP survey that ties Monell 180 ST 1. This provides an excellent image of the Upper Almond UA-5 reservoir, and also images the stratigraphic thickness variations in the

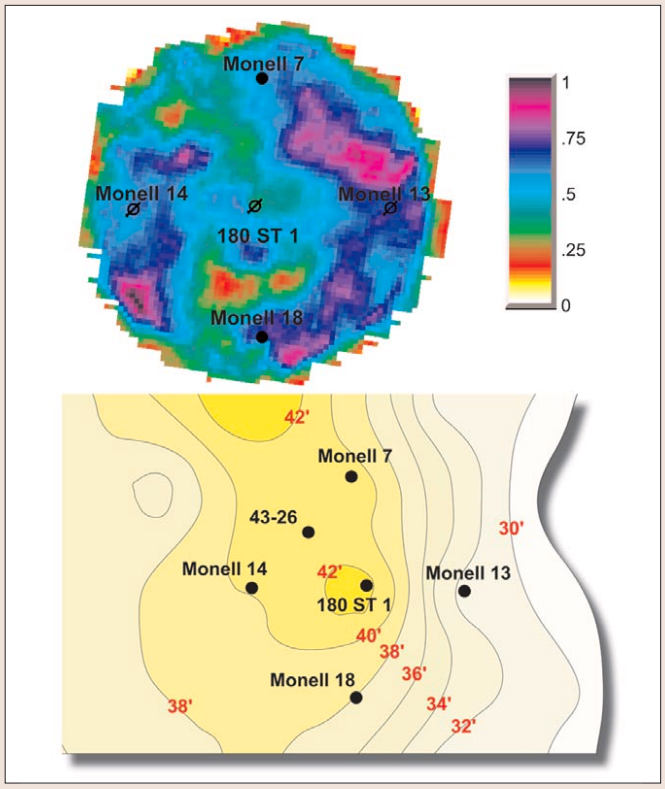

Figure 7. *Upper Almond Top UA-5 rms amplitude for baseline 3D VSP survey (top). Low amplitudes on the periphery are edge effects. UA-5 net sand thickness (bottom) based on well data, plotted with 2-ft contour interval. Higher amplitudes appear to correlate with thinner net sand thickness.*

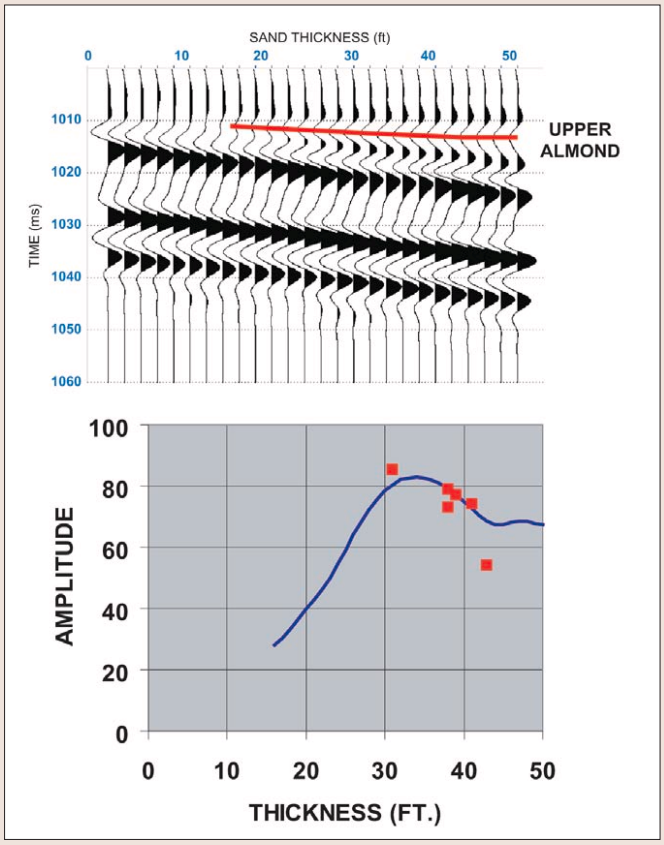

Figure 8. *Normal incidence wedge model for Upper Almond UA-5 sand saturated with brine/oil (top). Plot of Upper Almond UA-5 trough amplitude versus gross sand thickness(bottom) for wedge model (blue curve) and for the baseline VSP survey (red squares).*

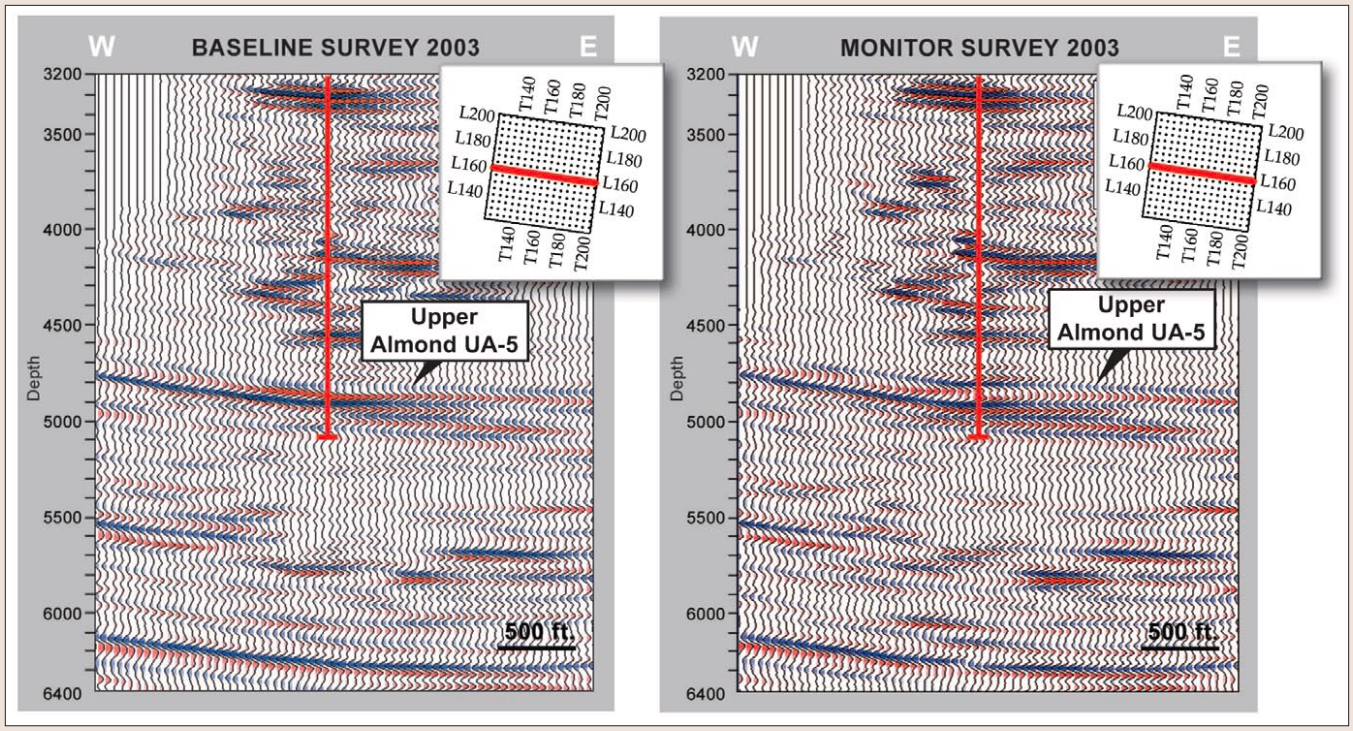

Figure 9. *Time-lapse comparison of east/west vertical section through Monell 180 ST 1 for baseline (left) and monitor (right) 3D VSP surveys.*

Upper Almond underlying the UA-5. The survey has a dominant wavelength of 80 ft in the zone of interest, measured directly from the depth section, showing the excellent vertical resolution achieved with this survey.

Figure 6 shows a profile from the VSP volume spliced into a coincident line from an overlying 3D seismic survey. The correlation between the two is excellent. While the surface seismic data have good bandwidth up to 60 Hz at these shallow depths, the VSP data have much higher frequency content and vertical resolution that provides more detailed imaging.

To assess the amplitude fidelity of the 3D VSP in the zone of interest, the Upper Almond Top UA-5 trough event was mapped. Figure 7 shows the corresponding amplitude map, based on an rms amplitude extraction over a 40-ft window encompassing the Top UA-5 event. Figure 7 also includes a UA-5 net sand thickness map based on well control.

The amplitude map shows a significant degree of character, even over this limited spatial area. Relative to the "background" amplitudes observed on the east and west sides of the survey, a ridge of lower amplitudes extends north-northwest from Monell 180 ST 1 while another area of lower amplitude is seen 600 ft south of the well. These appear to correlate with net sand thickness, higher amplitudes being associated with thinner net sand thickness.

This relationship can be evaluated further by comparing the measured VSP amplitudes with those predicted by seismic forward modeling. Figure 8 shows a normal-incidence wedge model based on log data from Monell 180 ST 1, where the thickness of the UA-5 sand has been modified in 2-ft increments per trace. The wavelet in this model has a frequency content that corresponds to the final migrated VSP survey. The lower display in Figure 8 compares the model amplitude response with the measured amplitudes at the six wells within the image area where sand thickness has been determined by the drill bit. This comparison is based on the five wells used in the pilot project and Monell 43-26 (drilled subsequently as part of the full-field EOR program). Comparing measured data and model results indicates that the UA-5 sand is at or above tuning thickness in the image area, and that reflection amplitude does indeed decrease with increasing sand thickness.

While sand thickness is identified as a major controlling factor in the amplitude response, the influence of variations in the underlying sand/shale/coal sequence cannot be ruled out. However, as these factors should be common to both baseline and monitor surveys, they are not expected to impact the time-lapse analysis.

To examine the time-lapse effects, Figure 9 compares an east/west vertical section on both the baseline and monitor surveys that ties Monell 180 ST 1:

- The two surveys show a high degree of similarity outside the reservoir interval that demonstrates the repeatability of the method.
- On the baseline survey, Upper Almond UA-5 shows a singlet trough which develops into a trough doublet in the vicinity of Monell 180 ST 1 due to increased sand thickness. The base of UA-5 is not resolved from reflections from the underlying coal-bearing section. This agrees closely with the synthetic seismogram in Figure 3.
- On the monitor survey, the upper trough of the doublet brightens significantly in the vicinity of the CO_2 injection well. This proves the most robust and most diagnostic time-lapse indicator. A change in character is also seen on the lower segment of the trough doublet; this is due to a change in the interference effects between reflections from the base of the UA-5 sand and the underlying coal-bearing section. The reflection from the base of the UA-5 sand has increased in amplitude due to the presence of CO_2 and the superposition pattern has been modified accordingly.

Differences between the two surveys can be evaluated more fully by subtracting the monitor depth-migrated volume from the baseline volume (Figure 10). Away from the injection well, the differences between the two surveys are incoherent and have low amplitude. In the vicinity of the well, the difference volume shows a strong trough response reflecting the brightening in amplitude of the Top UA-5

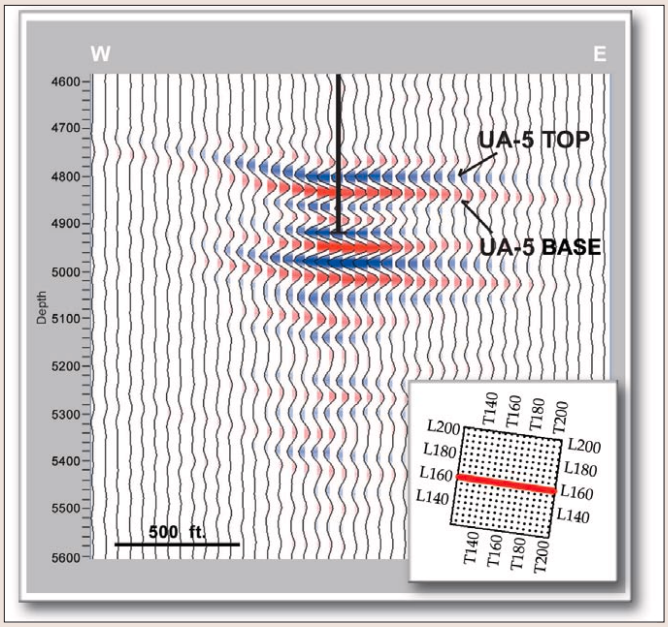

Figure 10. *Time-lapse 3D VSP east-west profile through Monell 180 ST 1 (monitor survey-baseline survey). Trace gain and vertical scale are twice that of Figure 9.*

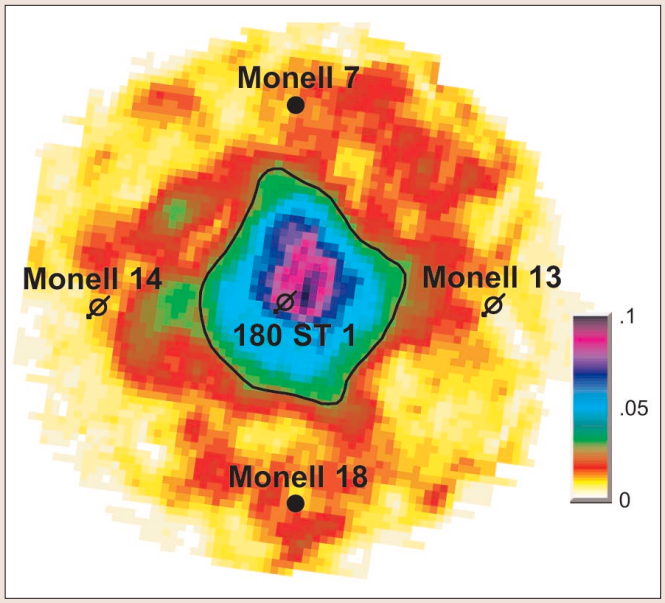

Figure 12. *Upper Almond UA-5 time-lapse amplitude map extracted from the difference of the cross-equalized volumes (monitor survey-baseline survey). Solid curve shows the interpreted CO_2 front. Monell 180 ST 1 is the CO_2 injection well and the well in which the 3D VSP surveys were acquired.*

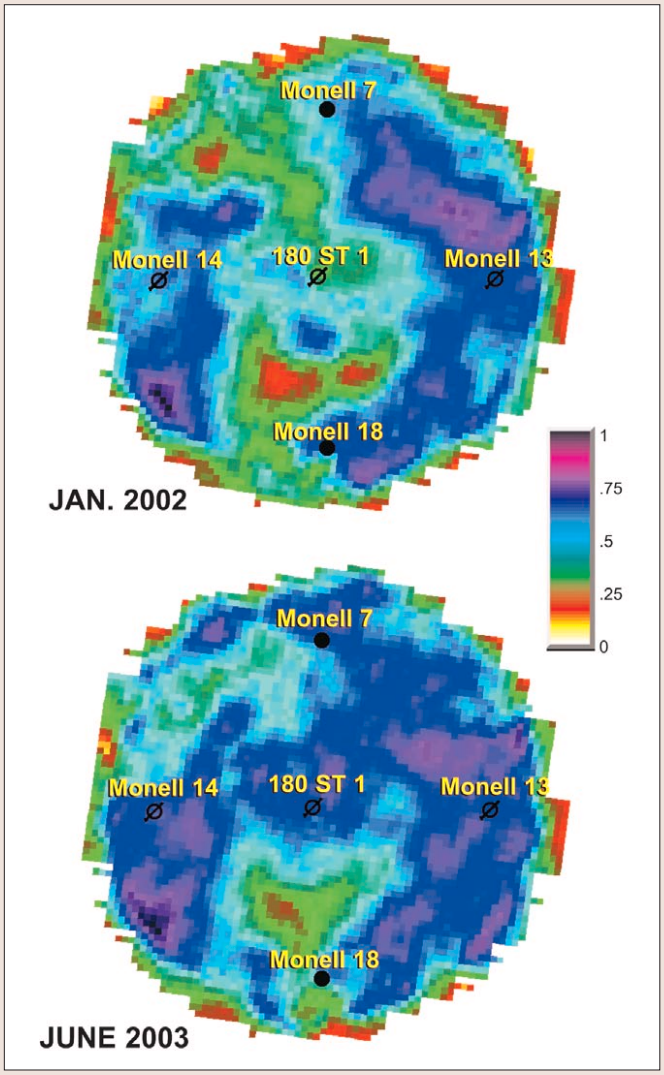

Figure 11. *The rms amplitude maps for the Upper Almond Top UA-5 reflection (trough) for the baseline survey (top) and monitor survey (bottom).*

trough event. This overlies a strong peak of comparable spatial extent which is associated with brightening of the Base UA-5 reflection due to CO_2 presence in the reservoir. It is interesting to note that the Base UA-5 event cannot be resolved on either the baseline or monitor surveys due to interference from the underlying coal-bearing sequence; however, these interference effects cancel out when we difference the two surveys and the Base UA-5 reflection can now be identified by its increase in amplitude due to CO_2 flooding.

The presence of CO_2 in the reservoir also causes a velocity push-down in the underlying reflections. This affects reflections immediately underlying the CO_2 flooded reservoir; deeper events are less affected by CO_2 in the reservoir and do not experience the same velocity push-down.

The velocity push-down causes a misalignment of events on the baseline and monitor surveys which gives rise to a set of events underlying the Base UA-5 peak on the difference volume. These are strictly velocity push-down effects as amplitudes of the corresponding events on the baseline and monitor surveys are comparable and also no CO_2 was injected at these deeper levels. Comparing the baseline and monitor surveys, the magnitude of the velocity push-down is measured as 6-8 ft which implies a decrease in P-wave velocity within the reservoir of 14-19% due to the CO_2 flood. This is greater than the change of 6% predicted by Biot-Gassmann equations; the difference may be due to uncertainties in pore fluid properties under reservoir conditions or inadequacies in the theory for multiphase fluids.

Figure 11 shows rms amplitude maps for the Upper Almond Top UA-5 trough event on the baseline and monitor surveys, based on a 40-ft window encompassing this event. Away from Monell 180 ST 1, we see a close similarity in the amplitude distributions. The striking feature of this comparison is the increase in amplitude on the monitor survey in the vicinity of Monell 180 ST 1, the CO_2 injection well, relative to the baseline survey.

Figure 12 shows the Upper Almond UA-5 time-lapse rms amplitude difference, picked on the volume which is the difference between the two cross-equalized surveys (monitor

- baseline). This amplitude extraction is based on the equivalent interval that is mapped in Figure 11 for the baseline and monitor surveys. The time-lapse 3-D VSP data clearly map the advance of the CO_2 front.

Time-lapse VSP data indicate that the CO_2 flood advanced 700-900 ft from the injector well, generally in a radial direction. There is some preference for CO_2 movement towards the north-northwest which is the updip direction. VSP data show good areal sweep efficiency with no indications of CO_2 channeling nor any areas that remain unswept behind the flood. The VSP results agree with production data recorded during the course of the pilot project (Table 4). During this time the two producing wells recorded increased oil production, with Monell Unit 7 (north) showing greater enhancement than Monell Unit 18 (south). No CO_2 breakthrough is observed in either well.

As production data provides information only at a few discrete locations, these data cannot tell us how far the CO_2 flood has advanced between wells or determine the shape of the CO_2 front. This is information that time-lapse VSP monitoring can provide; it can identify the spatial location of the CO_2 front, the configuration of the front and the areal sweep of the flood. These results can then be used for improved history-matching of the reservoir simulation model to improve the accuracy of predicting ultimate oil recovery and for better full field CO_2 flood performance predictions.

We can also obtain an estimate of the potential oil recovery of the pilot flood from the time-lapse data. Knowing the areal extent of the CO_2 front and the volume injected, we can estimate the CO_2 saturation within the reservoir. Assuming the flood extends over the full height of the reservoir and that saturation is uniform behind the flood front, mass balance calculations yield a CO_2 saturation of 15%. For a miscible flood, we can assume that CO_2 displaces an equal volume of oil in the reservoir. This indicates that an additional 28% of the original-oil-in-place is being displaced by the CO_2 flood in the pilot area, beyond that produced through primary or secondary recovery. Actual oil production will depend upon the flood continuing at the same efficiencies and the extent to which displaced or mobilized oil is recovered in producing wells.

Conclusions. 3D VSP imaging offers distinctive advantages that make it a powerful technique for time-lapse reservoir imaging. The high-frequency content of VSP data provides imaging detail with superior vertical and lateral resolution. The high signal/noise quality of the data yields images whose fidelity is sufficiently good that we can identify time-lapse effects with confidence and monitor changes in the reservoir. While the area imaged is small compared to that covered by a surface seismic survey, this may be sufficient for certain projects such as the Monell pilot project. Alternatively the technique may be expanded to a multiwell configuration.

In this paper we have presented a case study where time-lapse 3D VSP successfully imaged the Monell CO_2 pilot project with a level of detail which would not be available from surface seismic. Specific findings of this study are:

- 3D VSP imaged the Upper Almond reservoir with high vertical and lateral resolution and frequency content in excess of 130 Hz, and with high signal/noise ratio.
- Survey repeatability is excellent.
- The time lapse survey successfully monitored the CO_2 flood, showing that the CO_2 front moved a radial distance of 700 - 900 ft from the injector.
- The CO_2 flood is quite homogeneous, with a slight preference towards north-northwest (updip), in agreement with production data.

Table 4. *Production data for Monell CO_2 pilot project*

	Pre-CO_2 flood	Production after 18 months CO_2 flood
Monell 7	10 b/d	80 b/d
Monell 18	10 b/d	25 b/d

Time-lapse VSP aided significantly in evaluating the response of the reservoir to CO_2 injection, which was the primary goal of the pilot project. The impact of time-lapse monitoring can be summarized as follows:

- Provided direct and conclusive evidence of favorable CO_2 flood sweep efficiency.
- Shortened the evaluation time of the CO_2 pilot test.
- Provided input to reservoir simulations to predict tertiary oil recovery.
- Provided cost effective justification for proceeding with full field CO_2 flood, which requires large capital investment for new wells and facilities.

The full field CO_2 flood has now been launched and is being developed in a staged approach. Since the pilot is located within the full-flood area, a second monitor VSP survey is under consideration to ensure the expansion flood is behaving favorably within the pilot area.

Acknowledgments: We wish to thank Anadarko Petroleum Corporation for permission to present this paper. We also thank the many geoscientists at Anadarko and at P/GSI who contributed to the success of this project. The 3D VSP surveys were acquired and processed by P/GSI. Seismic data are from PGS data library and are shown courtesy of PGS Onshore, Inc.

Corresponding author: john_obrien@anadarko.com